



**HAL**  
open science

## A cis-antisense RNA acts in trans in *Staphylococcus aureus* to control translation of a human cytolytic peptide.

Nour Sayed, Ambre Jouselin, Brice Felden

### ► To cite this version:

Nour Sayed, Ambre Jouselin, Brice Felden. A cis-antisense RNA acts in trans in *Staphylococcus aureus* to control translation of a human cytolytic peptide.. *Nature Structural and Molecular Biology*, 2012, 19 (1), pp.105-12. 10.1038/nsmb.2193 . inserm-00696345

**HAL Id: inserm-00696345**

**<https://inserm.hal.science/inserm-00696345>**

Submitted on 1 Jul 2012

**HAL** is a multi-disciplinary open access archive for the deposit and dissemination of scientific research documents, whether they are published or not. The documents may come from teaching and research institutions in France or abroad, or from public or private research centers.

L'archive ouverte pluridisciplinaire **HAL**, est destinée au dépôt et à la diffusion de documents scientifiques de niveau recherche, publiés ou non, émanant des établissements d'enseignement et de recherche français ou étrangers, des laboratoires publics ou privés.

**A *cis* antisense RNA acts in *trans* in *Staphylococcus aureus* to control translation of a human cell damaging peptide.**

*Authors:* Nour Sayed, Ambre Jousselin & Brice Felden.

*Affiliations:* Biochimie Pharmaceutique Inserm U835 Upres EA2311 Université de Rennes,  
2 avenue du professeur Léon Bernard, 35000 Rennes, France.

Correspondence should be addressed to B.F. (bfelden@univ-rennes1.fr)

**Abstract**

Antisense RNAs (asRNAs) pair to RNAs expressed from the complementary strand, and their functions are thought to depend on nucleotide overlap with genes on the opposite strand. There is little information on their roles and mechanisms. We show that a *cis* asRNA acts in *trans*, utilizing a domain outside its target complementary sequence. SprA1 sRNA and SprA1<sub>AS</sub> asRNA are concomitantly expressed in *Staphylococcus aureus*. SprA1<sub>AS</sub> forms a complex with SprA1 preventing translation of the SprA1-encoded open reading frame by occluding translation initiation signals by pairing interactions. The SprA1 peptide sequence is within two RNA pseudoknots. SprA1<sub>AS</sub> represses production of the SprA1-encoded cytolytic peptide in *trans*, their overlapping region being dispensable for regulation. These findings demonstrate that, sometimes, asRNA functional domains are not their gene target complementary sequences, implying the need for mechanistic re-evaluations of asRNAs expressed in prokaryotes and eukaryotes.

## INTRODUCTION

In all living organisms, gene expression is modulated by proteins and small regulatory RNAs (sRNAs). sRNAs were identified in many bacteria and a few act by binding and modulating protein activity. The majority of sRNAs functions by pairing with target mRNAs, modifying mRNA transcription, stability or translation<sup>1</sup>. These base pairing sRNAs fall into two categories, *trans*- and *cis*-encoded sRNAs. The *trans* sRNAs are encoded at genomic locations distant from the mRNAs they regulate and share only limited complementarities with their targets. The *cis*-encoded antisense RNAs (asRNAs) are transcribed from the DNA strand opposite another gene and have perfect complementarities with their target. Recently, a considerable amount of natural asRNAs has been detected in various organisms, including human cells<sup>2</sup>.

In bacteria, antisense transcription was first demonstrated almost 50 years ago and was considered to be the exception to the rule. However, accumulating evidence from transcriptome studies suggests that extensive antisense transcription occurs in bacteria, producing many *cis*- sRNAs of various sizes<sup>3</sup>. In the human pathogen *Helicobacter pylori*, asRNAs were detected for 46% of all annotated open reading frames<sup>4</sup>, indicating that bacterial transcriptomes are unexpectedly complex. The functional relevance of this massive antisense transcription, however, is poorly understood but these asRNAs are predicted to have significant, as yet largely unexplored, impacts on gene expression. Also, information on the molecular mechanisms of individual asRNAs is growing at a slow pace. In bacteria, mechanisms of asRNA action include alteration of target RNA stability, transcription interference or termination, as well as translation modulation<sup>3</sup>.

The Gram-positive bacterium *Staphylococcus aureus* (*S. aureus*) is a major human pathogen causing a wide spectrum of nosocomial and community-associated infections with high mortality. *S. aureus* generates a large number of virulence factors whose timing and

expression levels are precisely tuned by regulatory proteins and sRNAs. *S. aureus* expresses at least 91 sRNAs<sup>5</sup> including asRNAs. Recent high-resolution transcriptome analysis detected a large proportion of these asRNAs among the inventoried *S. aureus* sRNAs<sup>6-9</sup>. In *S. aureus*, many asRNAs are expressed from Pathogenicity Islands (PIs) and mobile elements including plasmids and transposons. Since the SaPIs are the repository of toxins, adherence and invasion factors, superantigens and secretion systems, the location of sRNAs in the PIs suggests that they play important roles during *S. aureus* infections. In addition to all the *Small pathogenicity island rnas*<sup>6</sup> (RNAs expressed from the PIs), at least four asRNAs are also expressed from the PIs<sup>5</sup>. One of these asRNAs, Teg152, was detected in strain N315 by high throughput sequencing<sup>10</sup> and predicted, based on its overall genomic location, to be complementary with SprA1 3'-end. Because Teg152 acts as a functional asRNA against SprA1 as reported here, it was renamed SprA1<sub>AS</sub>. Sequence comparison suggest that the 'SprA1/SprA1<sub>AS</sub>' pair forms a type I 'toxin-antitoxin' (TA) module<sup>11</sup>. SprA1 was identified by computer searches combined with transcriptomic analysis and its expression verified by Northern blots<sup>6</sup>. The *sprA* gene is in 2–5 copies in the bacterial chromosome and in plasmids, depending on the strains. We set out to answer the question of the biological roles of the 'SprA1/SprA1<sub>AS</sub>' pair in *S. aureus*.

We provide evidence that a *cis*-encoded RNA functions in *trans*. During *S. aureus* growth, SprA1<sub>AS</sub> and SprA1 are constitutively and concomitantly expressed and the asRNA forms a complex with SprA1 *in vivo* to prevent internal translation of the SprA1-encoded open reading frame (ORF) by occluding its translation initiation signals by pairing interactions. Whereas the 60 nt-long SprA1<sub>AS</sub> is made of two stem-loops, the 208 nt-long SprA1 contains two RNA pseudoknots including an internal ORF. Polypeptide translation is naturally disfavoured by the SprA1 secondary structure in which its Shine-Dalgarno (SD) sequence is sequestered within a 5' stem-loop. The SprA1 peptide lyses human cells, and

upon SprA1<sub>AS</sub> binding, an internal RNA pseudoknot of SprA1 unfolds and forms a helix with SprA1<sub>AS</sub>. Structural evidences supported by mutational analysis of the RNAs indicate that the functional domain of SprA1<sub>AS</sub> is outside its 3'-complementary sequence with SprA1. Functional domains of antisense RNAs can be located outside from their target gene complementary sequences, rendering arduous mechanistic elucidations of asRNA-based gene regulation in all kingdoms of life.

## RESULTS

### Expression of SprA1 and SprA1<sub>AS</sub>

Up to five copies of *sprA* are detected in the *S. aureus* strains<sup>6</sup>. In strain Newman, a human clinical isolate, only two copies, *sprA1* and *sprA2*, are identified. Therefore, that strain is a simplified model for studying the multicopy *sprA* gene. In Newman, *sprA1* is located in the vSαβ pathogenicity island<sup>12</sup>, between a transposase and a hypothetical protein (Fig. 1a). We also detected an antisense RNA (asRNA) to SprA1, identified in strain N315 by high-throughput sequencing<sup>10</sup>. The *sprA1* and *sprA1<sub>AS</sub>* genes read in opposite directions with a predicted sequence overlap at their 3'-ends (Fig. 1a). A second copy, *sprA2*, is detected in the core genome at position '2560389-2560600', between a HP and a protein from the GtrA family (not shown). *SprA1* and *sprA2* share 74% nucleotide identity. Using a DNA probe specific of SprA1, we demonstrate that the RNA is expressed in Newman, as well as its asRNA, SprA1<sub>AS</sub>, (Fig. 1b). To distinguish between the expression of the two copies of *sprA*, and to assess their functional implications independently one another, a '*sprA1-sprA1<sub>AS</sub>*' deletion mutant ( $\Delta$ *sprA1-sprA1<sub>AS</sub>*) was constructed in Newman by homologous recombination. SprA1- and SprA1<sub>AS</sub>- specific DNA probes confirm the absence of expression of both SprA1 and SprA1<sub>AS</sub> in the deletion strain (Fig. 1b, right panel). Quantification of the expression levels of SprA1 and of SprA2 indicate that SprA1 is expressed two- to three-fold

more than SprA2 in the Newman strain (not shown). This report focuses on the functional investigation of the SprA1 and SprA1<sub>AS</sub> RNAs.

### **Nucleotide overlap between SprA1 and SprA1<sub>AS</sub>**

Determining SprA1 and SprA1<sub>AS</sub> 5' and 3' boundaries was required for subsequent functional and structural analysis. Since they are predicted to overlap, the extent of sequence overlay between the two RNAs was assessed experimentally in Newman. For SprA1, it was resolved using RACE (rapid amplification of cDNA ends), as described<sup>13</sup>, combined with direct size assessment using Northern blots on polyacrylamide gels (Fig. 1b, left panel).

SprA1 5'-end maps at position G<sub>1889597</sub> in strain Newman (at G<sub>1856485</sub> in strain N315, data not shown), twelve nucleotides downstream from a <sub>-12</sub>TATAAT<sub>.7</sub> box that is the predicted promoter (Supplementary Fig. 1a, boxed). SprA1 3'-end forms an intrinsic terminator characterized by a stem loop (H6, Supplementary Fig. 1a) followed by an imperfect U-tract (UUGGUGU). In *E. coli*, about half of the Rho-independent terminators possess imperfect U-tract<sup>14</sup>.

SprA1<sub>AS</sub> ends were very difficult to assess experimentally because its small size precludes from using RACE on circularized RNAs<sup>15</sup>. Therefore, SprA1<sub>AS</sub> transcriptional start site was resolved by primer extension analysis on total RNAs from wild-type Newman cells containing a pCN35ΩsprA1<sub>AS</sub> plasmid expressing SprA1<sub>AS</sub> from its endogenous promoter, to bypass the obstacle of its small size. We verified that SprA1<sub>AS</sub> expressed *in vivo* from the plasmid has a similar length that wild-type SprA1<sub>AS</sub>. SprA1<sub>AS</sub> 5'-end was assigned at position G<sub>1889770</sub> (Supplementary Fig. 2a). Therefore, SprA1<sub>AS</sub> 5'-end is positioned ten nucleotides downstream from a <sub>-10</sub>TATAAT<sub>.5</sub> box that is its predicted promoter (Supplementary Fig. 1b, boxed). SprA1<sub>AS</sub> 3'-end forms an intrinsic transcription terminator characterized by a stem loop (H2<sub>AS</sub>, Supplementary Fig. 1b) followed by a near-perfect U-tract (UUUUUAUU,

Supplementary Fig. 1b). SprA1<sub>AS</sub> is a ~60 nt-long asRNA. The experimental determination of the two RNA boundaries allowed producing them as synthetic transcripts.

### **Phylogenetic distribution of *sprA1* and *sprA1*<sub>AS</sub> genes**

The phylogenetic distribution of *sprA1* and *sprA1*<sub>AS</sub> was studied in all sequenced bacterial genomes. The genes encoding SprA1 and SprA1<sub>AS</sub> were identified in two orders of the bacilli class, the bacillales (*staphylococcaceae*, genus *staphylococcus*) and the lactobacillales (*enterococcaceae*, genus *enterococcus*). They were distinguished from *sprA2* that is in the core genome by their locations within the PIs. Sequence alignments of SprA1<sub>AS</sub> indicate sequence conservation in the non-overlapping region of the RNA pair, corresponding to ~20 nucleotides at the 5' side of the RNA. Within all the *aureus* species in which the RNA pair was detected, there is conservation of the two genes at the nucleotide level, suggesting selective pressure (Supplementary Fig. 1, only four *S. aureus* sequences shown). Within the *Staphylococcus* genus, however, there are differences scattered through the RNA sequence.

### **SprA1 and SprA1<sub>AS</sub> expression profiles during growth**

SprA1 and SprA1<sub>AS</sub> expression levels were monitored by northern blots during growth of *S. aureus* strain Newman (Fig. 1c and d). Their expression levels were quantified relative to tmRNA, a ubiquitous eubacterial sRNA expressed at constant levels during growth. SprA1 is constitutively expressed, detected early and present at all phases. SprA1<sub>AS</sub> is also expressed early and reproducibly exhibits a peak of expression at mid-exponential phase and is also expressed later. Similar expression patterns for the two RNAs are also observed in SH1000 and N315 *S. aureus* strains (data not shown). The *in vivo* concentrations of SprA1 and SprA1<sub>AS</sub> in wild-type Newman strain was determined by including a range of each of the purified synthetic RNAs in the Northern blots, for quantitative estimations (Fig. 1e). At all

times during growth, SprA1<sub>AS</sub> is in large excess relative to SprA1, from a 35- to a ~90 fold molar excess (Fig. 1e).

### ***In vivo* detection and binding of the ‘SprA1-SprA1<sub>AS</sub>’ duplex**

Since the two RNA genes are partially overlapping, we tested experimentally if the two RNAs, SprA1 and SprA1<sub>AS</sub> are interacting *in vivo*. For that purpose, a streptomycin-binding aptamer<sup>16</sup> was fused at the 5'-end of the *sprA1* gene and cloned into a ‘pCN35ΩST*sprA1*-*SprA1<sub>AS</sub>*’ plasmid expressing 5’ST-SprA1 (STSprA1) and SprA1<sub>AS</sub> from their endogenous promoters. The  $\Delta$ *sprA1*- $\Delta$ *sprA1<sub>AS</sub>* Newman strain was complemented with the ‘pCN35Ω ST*sprA1*-*sprA1<sub>AS</sub>*’ plasmid and Northern blots demonstrated that STSprA1 is expressed in the complemented strain at both mid-exponential (OD=3) and early stationary (OD=11) growth phases (Fig. 2a, STSprA1 is expressed to higher levels than wt SprA1 *in vivo* because of the plasmid copy number). As controls, the expression of SprA1 in wt cells, but not in the deletion strain, was monitored and the size difference between STSprA1 and wt SprA1 corresponds to the 46 nt-long ST. Total RNAs extracted from Newman ‘ $\Delta$ *sprA1*- $\Delta$ *sprA1<sub>AS</sub>*-pCN35Ω ST*sprA1*-*sprA1<sub>AS</sub>*’ cells were loaded on a streptomycin affinity matrix. As shown by PAGE (Supplementary Fig. 2b), the flow through (FT) contains the non specific RNAs (tRNAs and ribosomal RNAs), the last two washes cause some loss of STSprA1 from the column and, interestingly, the elution performed with 100 μM streptomycin contains STSprA1 and SprA1<sub>AS</sub> (Supplementary Fig. 2b), indicating that SprA1<sub>AS</sub> is in complex with immobilized STSprA1. As a negative control, total RNAs were extracted from Newman ‘WT-pCN35Ω*sprA1<sub>AS</sub>*’ cells and loaded onto the affinity matrix. Northern blots demonstrate that in the absence of STSprA1 *in vivo*, SprA1<sub>AS</sub> cannot bind the column by itself and is only detected in the FT, together with a non specific sRNA, tmRNA (Fig. 2b). However, with the ‘ $\Delta$ *sprA1*- $\Delta$ *sprA1<sub>AS</sub>*-pCN35Ω ST*sprA1*-*sprA1<sub>AS</sub>*’ cells, Northern blots demonstrate that the

eluted fraction contains both SprA1<sub>AS</sub> and STSprA1, but not tmRNA (Fig. 2b). Altogether, these experiments indicate that SprA1 forms a complex with SprA1<sub>AS</sub> *in vivo* and that its 5'ST does not hamper recognition.

Duplex formation between SprA1 and SprA1<sub>AS</sub> was analyzed by gel retardation assays. A 'SprA1-SprA1<sub>AS</sub>' duplex was detected at a 1:0.3 molar ratio and all SprA1 was in complex with sprA1<sub>AS</sub> at a 1:1 molar ratio (Fig. 2c). Complex formation between labeled SprA1 and SprA1<sub>AS</sub> was also analyzed and nearly all labeled SprA1 was in complex at a 1:1 molar ratio (Fig. 2d). In the two experiments, the binding is specific since a 1,000-fold molar excess of total tRNAs do not displace SprA1<sub>AS</sub> or SprA1 from preformed 'SprA1<sub>AS</sub>-SprA1' complexes, whereas a twenty-fold excess of unlabeled SprA1<sub>AS</sub> or SprA1 RNAs does. SprA1<sub>AS</sub> binds SprA1 with an apparent K<sub>d</sub> of 15nM ±5 (Fig. 2c and d), a value that was mandatory for complex formation between the two RNAs subsequently analyzed by structural probes in solution.

### **Structural interaction between SprA1 and SprA1<sub>AS</sub>**

We analyzed conformations of free SprA1 and SprA1<sub>AS</sub> (Supplementary Fig. 3), as well as the SprA1-SprA1<sub>AS</sub> duplexes (Supplementary Figs. 4 and 5) by structural probes (lead, RNase V1 and nuclease S1). The data are summarized onto SprA1 and SprA1<sub>AS</sub> models.

SprA1<sub>AS</sub> has two folded stems (H1<sub>AS</sub> and H2<sub>AS</sub>) separated by an 8 nt-long junction (H1-H2<sub>AS</sub>). Sequence alignments provide strong phylogenetic support for stem H1<sub>AS</sub>, but much less for H2<sub>AS</sub> (Supplementary Figs. 1b and 5b). In SprA1, the presence of V<sub>1</sub> cuts with no S<sub>1</sub> or lead cuts supports the existence of six stems, H1 to H6. Probing data support the existence of two loops, L1 and L6, capping respectively H1 and H6 (Supplementary Fig. 3b and c). Internal bulges within H1 and H6 are supported by nuclease S<sub>1</sub> and lead cleavages. A 5 nt junction separates H1 from the first pseudoknot, PK1 (H2-L2-H3-L3), followed by PK2 (H4-

L4 H5-L5). SprA1 is a compact RNA made of two tandem pseudoknots flanked by two stable helices, the second acting as a transcription terminator. Sequence alignments provide strong phylogenetic support for stem H1-H6 but not for H3 (Supplementary Figs. 1a and 5a).

The structural changes induced by duplex formation between the two RNAs were examined. Upon SprA1 binding, the most striking reactivity changes involve the single-stranded H1/H2<sub>AS</sub> junction that is cleaved by RNase V1 and protected from lead cuts, suggesting that it becomes double stranded upon duplex formation (Fig. 3, Supplementary Figs. 4 and 5c). An overall destabilization of the RNA is highlighted by the disappearance of V1 cuts in H1<sub>AS</sub> and H2<sub>AS</sub> as well as by the fading of S1 and lead cuts in L1<sub>AS</sub> and L2<sub>AS</sub>. Conversely, in the presence of SprA1<sub>AS</sub>, all the reactivity changes in SprA1 are centred between lower portion of H1 and PK1, indicating that it turns double-stranded, as it becomes protected from lead and S1 cuts (Fig. 3 and Supplementary Fig. 4a). Interestingly, there are no structural changes at the *cis*-overlapping region between the two RNAs. Altogether, the probing data collected on the ‘SprA1-SprA1<sub>AS</sub>’ duplex support an interaction between the two RNAs as presented on Figure 3. Comparing sequences from genomes and plasmids provides phylogenetic support of the interaction (covariations in Fig. 3b).

### **SprA1 and SprA1<sub>AS</sub> interact by non-overlapping domains**

Between SprA1 and SprA1<sub>AS</sub>, there is an intuitive binding site that involves a 35-nt overlap at their 3’-ends (Fig. 3c and d, yellow). Experimental evidences support a different, unexpected, binding site that involves pairings between nucleotides located at their 5’-domains (Fig. 3, red). To assess the contribution of those binding sites in duplex formation, SprA1 and SprA1<sub>AS</sub> were cleaved in two halves to retain a single binding domain on each RNA variant (‘5’-SprA1’, ‘3’-SprA1’, ‘5’-SprA1<sub>AS</sub>’ and ‘3’-SprA1<sub>AS</sub>’, Supplementary Fig. 6). Duplex formation between each of these shorter RNAs was analysed by gel retardation assays (Fig. 4

and Supplementary Fig. 2d). A specific '5'SprA1-SprA1<sub>AS</sub>' duplex is detected (Fig. 4a) with a  $K_d$  similar to that observed with wild-type SprA1 (Fig. 2c and d), whereas the 3'SprA1 construct is unable to bind SprA1<sub>AS</sub>, even at a 20 fold molar excess (Fig. 4b), indicating that SprA1 5'-domain, including H1-L1 and PK1, is necessary and sufficient to interact with SprA1<sub>AS</sub>. Also, a specific '5'SprA1<sub>AS</sub>-5'SprA1' duplex is detected (Supplementary Fig. 2d), with a weaker affinity than that between the two native RNAs (Fig. 2, c and d), probably because of two conformations for PK1 from 5'SprA1 (Supplementary Fig. 2d, two bands in the control lane) including an open and closed pseudoknotted structures. In addition, a specific '5'SprA1<sub>AS</sub>-SprA1' duplex is detected (Fig. 4c) but its apparent  $K_d$  is much higher than that between the two native RNAs, probably because of the reduced stability of 5'sprA1<sub>AS</sub> lacking the H2<sub>AS</sub> terminal helix, and also because of the reduced accessibility of the folded PK1 in full-length SprA1. Reciprocally, the 3'SprA1<sub>AS</sub> construct is unable to bind SprA1, even at a 200 fold molar excess (Fig. 4d). Overall, the non-overlapping 5'-domains of each RNA are necessary and sufficient for duplex formation, whereas the complementary 35 nucleotides at SprA1 and SprA1<sub>AS</sub> 3'-ends are dispensable for duplex formation.

### **Translation initiates onto SprA1 producing a peptide repressed by SprA1<sub>AS</sub> 5' non overlapping domain**

In all the *sprA1* genomic sequences, an internal ORF was identified (Supplementary Fig. 1a, green), predicted to encode a 30-33 amino acid-long peptide, starting at a <sub>51</sub>GUG<sub>53</sub> or <sub>54</sub>AUG<sub>56</sub> initiation codons and ending at a <sub>144</sub>UAG<sub>146</sub> stop codon. Moreover, an internally conserved '<sub>37</sub>AGGAGG<sub>42</sub>' Shine-Dalgarno (SD) sequence was identified 8 to 11 nucleotides upstream the predicted start codons (Fig. 5a). To test whether or not ribosomes can form translation initiation complexes onto SprA1, toeprint assays were performed on ternary initiation complexes including purified 70S ribosomes from *S. aureus*, initiator tRNA<sup>fMet</sup> and

SprA1. In the presence of the purified *S. aureus* ribosomes, toeprints are detected onto SprA1 at C65-C69 within L2 from pseudoknot PK1, 14 to 18 nucleotides downstream from the predicted initiation codons (Fig. 5b). The presence of multiple toeprints suggests that ribosome loading onto SprA1 takes place at several positions; probably because of two available initiation codons and also since there is a compact pseudoknot structure at the loading site that needs opening by the ribosomes. Within SprA1, the predicted SD sequence was mutated into  $_{37}\text{UCCUCC}_{42}$  and, to maintain the conformation of helix H1,  $_{5}\text{CCUAUCU}_{11}$  was also mutated into  $_{5}\text{GGAAGGA}_{11}$  (Fig. 5a). Ribosomes are unable to load onto this SprA1 variant named ‘SD-mutated sprA1’ (Fig. 5b, right panel), demonstrating that the  $_{37}\text{AGGAGG}_{42}$  sequence is required for translation initiation. Since the interaction between SprA1<sub>AS</sub> and SprA1 (Fig. 3) coincides with the region covered by the ribosomes during translation initiation, SprA1<sub>AS</sub> should prevent ribosome loading onto SprA1. Indeed, in the presence of SprA1<sub>AS</sub>, SprA1 toeprints disappear (Fig. 5b), indicating that the asRNA prevents ribosome loading onto SprA1. Interestingly, a strong stop is detected at U61 within SprA1 structure likely because RNA duplex formation induces a conformational change (Fig. 3).

*In vitro* translation assays were performed to provide direct experimental evidence that SprA1 can express a polypeptide predicted to contain 31 amino acids (Supplementary Fig. 7). In the presence of wild-type SprA1, a 2 to 5 KDa polypeptide is detected (Fig. 5c), in agreement with its ~3.45 KDa theoretical molecular weight. Remarkably, when SprA1<sub>AS</sub> is added in the reaction (2-fold molar excess compared to SprA1), SprA1 translation is blocked. We conclude that SprA1<sub>AS</sub> down regulates SprA1 translation by direct pairing interactions at and around the SprA1 translation initiation signals (Fig. 3). A ten-fold molar excess of either 5’SprA1<sub>AS</sub> or 3’SprA1<sub>AS</sub> was added in the translation assays of SprA1 (5’SprA1<sub>AS</sub> has a weaker binding affinity for SprA1 than wt SprA1<sub>AS</sub> has (Figs. 2c, 2d, and 4c). Whereas 5’SprA1<sub>AS</sub> reduces significantly SprA1 translation, 3’SprA1<sub>AS</sub> does not (Fig. 5c), providing

direct evidence that SprA1<sub>AS</sub> prevents SprA1 translation by its 5'-domain, but not by its 3'-domain. As a negative control, the 'SD-mutated SprA1' cannot be translated *in vitro* (Fig. 5c), in agreement with the toeprint data, as it fails to recruit the *S. aureus* ribosomes (Fig. 5b, right panel). Altogether, these experiments indicate that SprA1<sub>AS</sub> binds SprA1 at its 5' non-overlapping sequence to block internal translation of SprA1. To assay if SprA1<sub>AS</sub> also regulates SprA1 transcription and/or stability, in addition to its translational control, SprA1<sub>AS</sub> was over expressed *in vivo* and the expression levels of SprA1 were monitored by northern blots during bacterial growth. Increasing the expression levels of SprA1<sub>AS</sub> does not significantly affect SprA1 levels *in vivo*, ruling out a direct regulation at the RNA level (Fig. 5d).

#### **SprA1-encoded peptide expression is down regulated *in trans* by cis-SprA1<sub>AS</sub> *in vivo***

With regard to the data presented above, the *sprA1* and *sprA1<sub>AS</sub>* genes were linked physically. Decoupling genetically the location and expression of the two overlapping RNAs was required to demonstrate *in vivo* that a cis-sRNA operates in *trans*. The SprA1 peptide has very low immunogenicity (not shown), and its over expression *in vivo* inhibits *S. aureus* growth (data not shown). A reporter peptide construct was designed by combining the 5'-sequence of SprA1 including 20 amino acids at N-ter from its internal coding sequence, merged to a 22 amino acid 3XFlag, for detection. SprA1 peptide truncation of its 11 amino acids at C-ter was required to lower its toxicity *in vivo*. Also, the transcription terminator sequence of SprA1 that overlaps with *sprA1<sub>AS</sub>* was replaced by another unrelated terminator sequence (*blaZ*). A low-copy (~20 copies per bacterium) vector was used (pCN34) and the pCN34Ω*sprA1tag* was transformed into Newman Δ*sprA1*-Δ*sprA1<sub>AS</sub>*. Immunoblots using anti-FLAG antibodies demonstrate that the SprA1 fusion peptide is expressed *in vivo* (Fig. 6a). To monitor the impact of SprA1<sub>AS</sub> on the SprA1-encoded fusion peptide *in vivo*, strain Δ*sprA1*-

$\Delta sprA1_{AS}$  pCN34 $\Omega sprA1tag$  was transformed with either pCN35 or pCN35 $\Omega sprA1_{AS}$ . In the strain containing the two RNAs in *trans*, each expressed from a different plasmid, SprA1 peptide levels are drastically reduced (Fig. 6a), demonstrating the down regulation of the expression of the SprA1 peptide by SprA1<sub>AS</sub> *in vivo*. Northern blots validate the presence of the SprA1-flagged and SprA1<sub>AS</sub> RNAs in the ' $\Delta sprA1-\Delta sprA1_{AS}$ ' double deletion strain containing the two plasmids whereas, as expected, there is only the SprA1-flagged RNA in the  $\Delta sprA1-\Delta sprA1_{AS}$  pCN34 $\Omega sprA1tag$  strain transformed with the empty pCN35 plasmid (Fig. 6b). We conclude that SprA1<sub>AS</sub> prevent sprA1-encoded peptide expression in *trans in vivo* and that its 3'-overlapping region with SprA1 is dispensable for the regulation.

### **The SprA1-encoded peptide is cytolytic for human cells**

Sequence alignments of the SprA1-encoded peptide indicate  $\alpha$ -helicity and amphipathy (Supplementary Fig. 7), which are typical features of pore-forming peptides<sup>17</sup>. The lytic activity of the SprA1 peptide was demonstrated by adding increasing concentrations of the chemically synthesized peptide on human erythrocytes (Fig. 7a). The SprA1 peptide lyses human erythrocytes at a 1 $\mu$ M concentration and above, but is less active towards sheep erythrocytes (Fig. 7b), suggesting a narrow hemolytic range. Some microbial hemolysins display antibacterial activity<sup>18</sup>. The SprA1 peptide has also antimicrobial activity against Gram negative and positive bacteria (not shown). The bactericidal activity of the SprA1 peptide against *S. aureus* cells gives a rationale as to why SprA1<sub>AS</sub> is continuously expressed during bacterial growth, preventing SprA1 translation and toxicity against *S. aureus* cells.

## **DISCUSSION**

Many asRNAs were recently inventoried in bacteria and eukaryotes but information on the molecular mechanisms underlying their functions is, for the most part, unknown. By

definition, *cis*-asRNAs regulate the genes encoded on the respective opposite strands<sup>19</sup>. It is commonly accepted that *cis*-asRNA functions are linked to their sequence overlap with genes transcribed from the opposite DNA chain. We report a case of an asRNA that acts as a *trans* regulator in *S. aureus*. It demonstrates that asRNAs can interact in *trans* with complementary target genes and possibly also with other genes at remote genetic loci. Base complementarities between overlapping RNAs do not necessarily imply that they are the functional unit of the pair. Because *cis*-RNAs can work in *trans*, the distinction between *cis*- and *trans*- RNAs should be revised. Our findings also suggest that the mechanisms of gene regulations of the identified asRNAs should be re-evaluated, as some could operate in *trans* on targets. It may be advantageous for *trans* sRNAs to be located in *cis* on the chromosome because, during genomic rearrangements, they will move with their target genes. In many bacteria, *trans*-acting sRNAs require the Hfq RNA chaperone protein for pairings with target RNAs<sup>20</sup>. *In vivo*, SprA1 steady-state levels are unaffected by the presence or absence of Hfq (Supplementary Fig. 2c), suggesting that the protein is dispensable for the interaction between SprA1<sub>AS</sub> and SprA1. The *cis*-overlap between SprA1 and SprA1<sub>AS</sub> 3'-ends operates as a bi-directional transcription terminator, presumably for genome compaction and tightness. Their 5' non-overlapping domains, however, interact in *trans* to repress SprA1-encoded cytolytic peptide synthesis (Fig. 7c).

SprA1 has a compact secondary structure made of RNA pseudoknots flanked by stable stem-loops, hindering internal translation initiation signals from the ribosomes. Despite such structural lock, the *S. aureus* ribosomes can load onto SprA1 *in vitro* to produce a 31 amino acid peptide. SprA1<sub>AS</sub> is therefore required to block internal translation onto SprA1, inducing a conformation rearrangement by pairing interactions. These observations are consistent with a continuous and tight repression of peptide synthesis that is detrimental for *S. aureus* growth (data not shown). The SprA1 peptide is probably only expressed under restricted, currently

unknown, physiological conditions by specific environmental clue(s) reducing SprA1<sub>AS</sub> levels. The peak of SprA1<sub>AS</sub> expression at mid-exponential phase suggests that translation repression of SprA1 is optimized during the exponential phase, probably to insure that the lytic peptide is not produced when the *S. aureus* cells are actively spreading. Alternatively, SprA1<sub>AS</sub> could have other functions; it might act in *trans* on other RNAs. Indeed, in *Listeria monocytogenes*, riboswitches that are *cis*-RNA elements can also function in *trans*, therefore acting as regulatory RNAs<sup>21</sup>. SprA1 could have other functions, possibly at the RNA level, in addition to expressing a peptide. Dual functions, at the transcription and translation levels, were recently reported for a cytolysin (phenol-soluble modulin, PSM) regulating virulence in *S. aureus*<sup>22</sup>.

The SprA1 peptide is a novel virulence factor that lyses erythrocytes and probably other eukaryotic cell types and organelles, possibly also involved in erasing competing bacteria. Its function is consistent with its genomic location within a PI-containing virulence gene. In order to exert its cytotoxicity, the SprA1 peptide should be released from the bacteria. Another *S. aureus* cytolytic peptide, the  $\delta$ -hemolysin<sup>23</sup>, is internally encoded within a sRNA, RNAIII.  $\delta$ -hemolysins are  $\alpha$ -helical and amphipatic PSMs, as the SprA1 peptide (Supplementary Fig. 7), and active against a wide range of cells and organelles.  $\delta$ -hemolysin enables the phagosomal escape of staphylococci in human cells<sup>24</sup>. Therefore, the SprA1 peptide could also be involved in evading the human phago-endosomes, the acidic pH could lower SprA1<sub>AS</sub> levels, leading to SprA1 peptide expression.

Based on sequence comparisons, SprA1 and SprA1<sub>AS</sub> were proposed to form a type I TA module resembling those of the LDR/Fts family<sup>11</sup>. Type-I TA modules kill cells usually by forming pores<sup>11</sup>, some are involved in the general stress response<sup>25</sup> or in specific functions including controlling production of multidrug tolerant cells<sup>26</sup>. Here, the toxin is internally encoded by a sRNA and not by an mRNA, and protein synthesis is prevented by the sRNA

antitoxin in *trans*. Bacterial Type-I TA systems are usually found in multiple copies and there is up to five copies of *sprA* in some *S. aureus* strains<sup>6</sup>, but the systematic expression of an associated asRNA with each copy is unknown. However, one difference between the TA systems and ‘SprA1-SprA1<sub>AS</sub>’ is that *in vivo*, SprA1 levels are unaffected by increasing SprA1<sub>AS</sub> expression. The SprA1-encoded peptide shares physico-chemical properties with *S. aureus* PSMs that are small, amphipathic and  $\alpha$ -helical peptides with significant cytolytic activity against human neutrophils and erythrocytes<sup>27</sup>.  $\alpha$ -type PSMs also cause chemotaxis and cytokines release. Therefore, similar biological activities are anticipated for the SprA1 peptide. PSMs are regulated by the accessory gene regulator A through its direct interaction with the PSM promoter<sup>28</sup>. In contrast, SprA1 translation is down-regulated by an asRNA, as for the TA systems.

In conclusion, *cis* antisense RNAs can officiate in *trans*, implying mechanistic re-evaluations of the identified antisense RNA-mediated target gene regulations in eubacteria, archeas and eukaryotes. Also, a novel virulence factor expressed by *S. aureus* is reported and its expression is locked *in vivo* by an inhibitory sRNA pair. The next challenges are to understand when this novel cytolytic is expressed and what its biological functions are during staphylococcal infections.

## REFERENCES

1. Waters, L.S. & Storz, G. Regulatory RNAs in bacteria. *Cell* **136**, 615-28 (2009).
2. He, Y., Vogelstein, B., Velculescu, V.E., Papadopoulos, N. & Kinzler, K.W. The antisense transcriptomes of human cells. *Science* **322**, 1855-7 (2008).
3. Georg, J. & Hess, W.R. cis-Antisense RNA, Another Level of Gene Regulation in Bacteria. *Microbiol Mol Biol Rev* **75**, 286-300 (2011).
4. Sharma, C.M. et al. The primary transcriptome of the major human pathogen *Helicobacter pylori*. *Nature* **464**, 250-5 (2010).
5. Felden, B., Vandenesch, F., Bouloc, P. & Romby, P. The *Staphylococcus aureus* RNome and its commitment to virulence. *PLoS Pathog* **7**, e1002006 (2011).
6. Pichon, C. & Felden, B. Small RNA genes expressed from *Staphylococcus aureus* genomic and pathogenicity islands with specific expression among pathogenic strains. *Proc Natl Acad Sci U S A* **102**, 14249-54 (2005).
7. Abu-Qatouseh, L.F. et al. Identification of differentially expressed small non-protein-coding RNAs in *Staphylococcus aureus* displaying both the normal and the small-colony variant phenotype. *J Mol Med* **88**, 565-75 (2010).
8. Geissmann, T. et al. A search for small noncoding RNAs in *Staphylococcus aureus* reveals a conserved sequence motif for regulation. *Nucleic Acids Res* **37**, 7239-57 (2009).
9. Bohn, C. et al. Experimental discovery of small RNAs in *Staphylococcus aureus* reveals a riboregulator of central metabolism. *Nucleic Acids Res* **38**, 6620-36 (2010).
10. Beaume, M. et al. Cartography of methicillin-resistant *S. aureus* transcripts: detection, orientation and temporal expression during growth phase and stress conditions. *PLoS One* **5**, e10725 (2010).

11. Fozo, E.M. et al. Abundance of type I toxin-antitoxin systems in bacteria: searches for new candidates and discovery of novel families. *Nucleic Acids Res* **38**, 3743-59 (2010).
12. Baba, T., Bae, T., Schneewind, O., Takeuchi, F. & Hiramatsu, K. Genome sequence of *Staphylococcus aureus* strain Newman and comparative analysis of staphylococcal genomes: polymorphism and evolution of two major pathogenicity islands. *J Bacteriol* **190**, 300-10 (2008).
13. Antal, M., Bordeau, V., Douchin, V. & Felden, B. A small bacterial RNA regulates a putative ABC transporter. *J Biol Chem* **280**, 7901-8 (2005).
14. Peters, J.M., Vangeloff, A.D. & Landick, R. Bacterial Transcription Terminators: The RNA 3'-End Chronicles. *J Mol Biol* (2011) doi:10.1016/j.jmb.2011.03.036.
15. Redko, Y., Bechhofer, D.H. & Condon, C. Mini-III, an unusual member of the RNase III family of enzymes, catalyses 23S ribosomal RNA maturation in *B. subtilis*. *Mol Microbiol* **68**, 1096-106 (2008).
16. Windbichler, N. & Schroeder, R. Isolation of specific RNA-binding proteins using the streptomycin-binding RNA aptamer. *Nat Protoc* **1**, 637-40 (2006).
17. Mellor, I.R., Thomas, D.H. & Sansom, M.S. Properties of ion channels formed by *Staphylococcus aureus* delta-toxin. *Biochim Biophys Acta* **942**, 280-94 (1988).
18. Verdon, J., Girardin, N., Lacombe, C., Berjeaud, J.M. & Hechard, Y. delta-hemolysin, an update on a membrane-interacting peptide. *Peptides* **30**, 817-23 (2009).
19. Thomason, M.K. & Storz, G. Bacterial antisense RNAs: how many are there, and what are they doing? *Annu Rev Genet* **44**, 167-88 (2010).
20. Chao, Y. & Vogel, J. The role of Hfq in bacterial pathogens. *Curr Opin Microbiol* **13**, 24-33 (2010).

21. Loh, E. et al. A trans-acting riboswitch controls expression of the virulence regulator PrfA in *Listeria monocytogenes*. *Cell* **139**, 770-9 (2009).
22. Kaito, C. et al. Transcription and translation products of the cytolysin gene *psm-mec* on the mobile genetic element SCCmec regulate *Staphylococcus aureus* virulence. *PLoS Pathog* **7**, e1001267 (2011).
23. Janzon, L., Lofdahl, S. & Arvidson, S. Identification and nucleotide sequence of the delta-lysin gene, *hld*, adjacent to the accessory gene regulator (*agr*) of *Staphylococcus aureus*. *Mol Gen Genet* **219**, 480-5 (1989).
24. Giese, B. et al. Expression of delta-toxin by *Staphylococcus aureus* mediates escape from phago-endosomes of human epithelial and endothelial cells in the presence of beta-toxin. *Cell Microbiol* **13**, 316-29 (2011).
25. Wang, R. et al. Identification of novel cytolytic peptides as key virulence determinants for community-associated MRSA. *Nat Med* **13**, 1510-4 (2007).
26. Dorr, T., Vulic, M. & Lewis, K. Ciprofloxacin causes persister formation by inducing the TisB toxin in *Escherichia coli*. *PLoS Biol* **8**, e1000317 (2010).
27. Otto, M. Basis of virulence in community-associated methicillin-resistant *Staphylococcus aureus*. *Annu Rev Microbiol* **64**, 143-62 (2010).
28. Queck, S.Y. et al. RNAIII-independent target gene control by the *agr* quorum-sensing system: insight into the evolution of virulence regulation in *Staphylococcus aureus*. *Mol Cell* **32**, 150-8 (2008).
29. Charpentier, E. et al. Novel cassette-based shuttle vector system for gram-positive bacteria. *Appl Environ Microbiol* **70**, 6076-85 (2004).
30. Chabelskaya, S., Gaillot, O. & Felden, B. A *Staphylococcus aureus* small RNA is required for bacterial virulence and regulates the expression of an immune-evasion molecule. *PLoS Pathog* **6**, e1000927 (2010).

31. Bruckner, R. Gene replacement in *Staphylococcus carnosus* and *Staphylococcus xylosus*. *FEMS Microbiol Lett* **151**, 1-8 (1997).
32. Cheung, A.L., Eberhardt, K.J. & Fischetti, V.A. A method to isolate RNA from gram-positive bacteria and mycobacteria. *Anal Biochem* **222**, 511-4 (1994).
33. Schagger, H. Tricine-SDS-PAGE. *Nat Protoc* **1**, 16-22 (2006).

## FIGURE LEGENDS

### Figure 1 Genomic location, lengths, boundaries, and expression of *sprA1* and *sprA1<sub>AS</sub>*.

(a) Location of *sprA1/sprA1<sub>AS</sub>* in Pathogenicity Island *SaPI<sub>n3</sub>* of *S. aureus* strain Newman genome. (b) Right panels: Northern blots detection of SprA1 and SprA1<sub>AS</sub> in a wild-type Newman strain (lane 1) and in an isogenic *sprA1/sprA1<sub>AS</sub>* double deletion strain (lane 2). Left panels: Lengths evaluation of SprA1 and SprA1<sub>AS</sub> adjoining synthetic labeled RNAs of known lengths combined to 5'-end determinations by RACE mapping. The nucleotide numberings of SprA1 and SprA1<sub>AS</sub> ends refer to positions in *S. aureus* Newman genomic sequence<sup>12</sup>. (c-d) SprA1 and SprA1<sub>AS</sub> expression profiles during *S. aureus* growth. The expression levels of SprA1 and SprA1<sub>AS</sub> during a 10-hour growth of *S. aureus* Newman strain detected by Northern blots. As loading controls, the blots were also probed for tmRNA. The growth curves of the Newman strain is presented, with the quantification of SprA1 (black triangles) and SprA1<sub>AS</sub> (grey diamonds) levels relative to the amount of tmRNA from the same RNA extraction. AU =arbitrary units. (e) Determination of the *in vivo* concentrations of SprA1 and SprA1<sub>AS</sub> in a wild-type *S. aureus* Newman strain during growth detected by Northern blots. The quantification of SprA1 and SprA1<sub>AS</sub> *in vivo* levels (left panels) were performed relative to increasing amounts of synthetic, gel purified SprA1 and SprA1<sub>AS</sub> RNAs (the two right panels). *In vivo*, the ratios between the SprA1 and SprA1<sub>AS</sub> RNAs are 1/35, 1/92, 1/63 and 1/50, respectively at A<sub>600nm</sub> of 4, 7, 10 and 12.

### Figure 2 Detection of the interaction between SprA1 and SprA1<sub>AS</sub> *in vivo* and assessing their binding constants.

(a) Northern blot analysis of SprA1 (wild-type or tagged with a ST) expression at mid-exponential (OD<sub>600nm</sub> = 3) and stationary (OD<sub>600nm</sub> = 11) phases in Newman wild-type (lane 3), isogenic Newman  $\Delta$ *sprA1/sprA1<sub>AS</sub>* deletion mutant (lane 2) and Newman  $\Delta$ *sprA1*- $\Delta$ *sprA1<sub>AS</sub>* *pCN35 $\Omega$ STsprA1/sprA1<sub>AS</sub>* strain (lane 1). (b) Northern blot

analysis of the affinity purification fractions from either Newman  $\Delta sprA1-\Delta sprA1_{AS}$   $pCN35\Omega STsprA1/sprA1_{AS}$  extracts, or Newman wild-type  $pCN35\Omega sprA1_{AS}$  extracts, as a negative control. Labeled DNA probes were used for SprA1 (WT and tagged), for SprA1<sub>AS</sub> and for tmRNA used as an internal negative control. FT = flow through, W4 = wash 4, W5 = wash 5, E = elution. **(c,d)** Complex formation between purified SprA1 and SprA1<sub>AS</sub> by native gel retardation assays. Purified labeled (asterisks) SprA1<sub>AS</sub> **(c)** or SprA1 **(d)** with increasing amounts of unlabeled SprA1 **(c)** or unlabeled SprA1<sub>AS</sub> **(d)**. The diamonds indicate the molar ratios used to perform the competition assays with a 1000-fold molar excess of *yeast* total tRNAs or with a 20-fold molar excess of the indicated unlabeled RNA. The apparent binding constant between SprA1<sub>AS</sub> and SprA1 was inferred from these data:  $K_d = 15 \pm 5$  nM.

**Figure 3 Experimental and phylogenetic evidence for the pairings between SprA1<sub>AS</sub> and SprA1.** **(a)** Proposed pairings between SprA1 and SprA1<sub>AS</sub>. SD and GUG/AUG start codons are in red, the SprA1<sub>AS</sub> and SprA1 interacting domains are boxed in red. Blue minus signs indicate the disappearance of the cleavages triggered by the structural probes in the RNA duplex. Triangles are the V1 cuts, arrows capped by circles are the S1 cuts and uncapped arrows are the lead cleavages. The intensity of the cleavages is proportional to the darkness of the symbols. The blue S1 cut appears when the duplex forms. **(b)** Phylogenetic support for the proposed interaction between SprA1 and SprA1<sub>AS</sub> when comparing the sequences of the two RNAs located in genomes and plasmids. Covariations are shown in grey, SD and start codons are boxed. **(c,d)** Experimentally supported structure of SprA1 and SprA1<sub>AS</sub> emphasizing the 3'-overlapping sequence (yellow) as well as the experimentally and phylogenetically supported interaction region (red box). Covariations are shown in grey. The other symbols are similar to panel **(a)**. Structural changes detected upon complex formation are indicated in blue. The domains of the RNAs are indicated (SprA1: H1-H6, H1-H2

junction, L1-L6, PK1-PK2; SprA1<sub>AS</sub>: H1-H2<sub>AS</sub>, H1<sub>AS</sub>-H2<sub>AS</sub> junction and L1<sub>AS</sub>-L2<sub>AS</sub>). See also Supplementary Figs. 3-5.

**Figure 4 SprA1 and SprA1<sub>AS</sub> interact by their 5' non-overlapping domains.** Complex formation between labeled SprA1<sub>AS</sub> with increasing amounts of unlabeled 5'SprA1 **(a)** or 3'SprA1 **(b)** and between labeled SprA1 with increasing amounts of unlabeled 5'SprA1<sub>AS</sub> **(c)** or 3'SprA1<sub>AS</sub> **(d)**, detected by native gel retardation assays. The apparent binding constants between the RNAs were inferred from these data. For 'SprA1<sub>AS</sub>-5'SprA1', the K<sub>d</sub> is 16 ± 5nM. For 'SprA1-5'SprA1<sub>AS</sub>', the K<sub>d</sub> is 300 ± 50nM. There is no duplex formation between SprA1 and 3'SprA1<sub>AS</sub> or between 3'SprA1 and SprA1<sub>AS</sub>. The black diamonds indicate the molar ratios used to perform the competition assays with a 2000-fold molar excess of polyU RNAs or with a 20-fold molar excess of indicated unlabeled RNA. Asterisks point to the <sup>32</sup>P-radiolabeled RNAs. See also Supplementary Fig. 6.

**Figure 5 SprA1 recruits the *S. aureus* ribosomes, is translated *in vitro* and SprA1<sub>AS</sub> hinders SprA1 translation by its 5' non-overlapping domain.** **(a)** SprA1 structure indicating the ribosome toeprints (oval), the reverse transcriptase (RT) pause in the presence of sprA1<sub>AS</sub> (black arrowhead) and the mutated nucleotides in the 'SD-mutated SprA1' construct (rectangles, twelve mutated nucleotides to maintain H1 while modifying the SD sequence). The predicted initiation and termination codons are framed and the nucleotide sequence overlapping with sprA1<sub>AS</sub> is in grey. **(b)** *S. aureus* ribosome toeprints onto SprA1 (WT SprA1), and the disappearance of the toeprints onto the 'SD-mutated SprA1'. In the presence of SprA1<sub>AS</sub> at a 2:1 molar ratio, there are no toeprints, indicating that the asRNA impairs ribosome loading onto SprA1. The toeprints are indicated with a black bar and the RT pause onto SprA1, in the presence of SprA1<sub>AS</sub>, is indicated by an arrowhead. 'T', 'A', 'G'

and 'C' are the SprA1 sequencing ladders. **(c)** *In vitro* translation of SprA1 (lane 1), of SprA1 in the presence of SprA1<sub>AS</sub> at a 1:1 molar ratio (lane 2), of SprA1 in the presence of 5'SprA1<sub>AS</sub> at a 1:10 molar ratio (lane 3), of SprA1 in the presence of 3'SprA1<sub>AS</sub> at a 1:10 molar ratio (lane 4), of SD-mutated SprA1 (lane 5). The translated 'SprA1-encoded' polypeptide of ~3kDa is indicated by an arrowhead. **(d)** Northern blot analysis of SprA1 and SprA1<sub>AS</sub> in Newman pCN35 and isogenic Newman pCN35 $\Omega$ sprA1<sub>AS</sub> during growth. 5S rRNAs are the controls.

**Figure 6 SprA1<sub>AS</sub> *cis* RNA acts *in trans* to down-regulate SprA1-encoded peptide expression *in vivo*.** **(a)** Detection of the ~5kDa SprA1-encoded flagged peptide at early (OD<sub>600nm</sub>=1) and mid-exponential (OD<sub>600nm</sub>=5) phases of growth in strains Newman ' $\Delta$ sprA1- $\Delta$ sprA1<sub>AS</sub> pCN34 $\Omega$ sprA1tag pCN35' (lanes 1 and 3) and in isogenic Newman ' $\Delta$ sprA1- $\Delta$ sprA1<sub>AS</sub> pCN34 $\Omega$ sprA1tag pCN35 $\Omega$ sprA1<sub>AS</sub>' strain (lanes 2 and 4) by immunoblots using anti-FLAG antibodies. **(b)** Northern blot analysis monitoring SprA1-FLAG RNA (upper panel) and SprA1<sub>AS</sub> RNA (lower panel) expression levels at identical phases of growth. 5S rRNAs are the internal loading controls.

**Figure 7 The SprA1-encoded peptide is lytic for human cells.** **(a)** Hemolytic activity of synthetic SprA1-encoded peptide compared to a non-hemolytic peptide used as a negative control. Controls: the minus sign indicates that PBS was added to the RBCs, the plus sign indicates hypotonic solution was added to RBCs. RBC sedimentation indicates the absence of hemolysis, whereas a red supernatant implies hemolysis. **(b)** Differential hemolytic activity of the synthetic SprA1 peptide between human and sheep RBCs. The peptide induces a strong hemolysis on the human RBCs but a weak hemolysis on the sheep RBCs. **(c)** Proposed model for the down-regulation of SprA1 sRNA internal translation *in trans* by the *cis*-

encoded SprA1<sub>AS</sub>. The SprA1 internal ORF is shown in green and the SprA1 and SprA1<sub>AS</sub> 5' non-overlapping interacting domains are in red. Their 3'-overlapping domains are in yellow. Upon duplex formation, SprA1<sub>AS</sub> 5' domain pairs at and around the SprA1 internal translation initiation signals (SD sequence and start codon, red) by unfolding pseudoknot PK1. During *S. aureus* growth, translation of the SprA1-encoded peptide is repressed by base pairings in *trans* with SprA1<sub>AS</sub> RNA. See also Supplementary Fig. 7.

## METHODS

### Strains and plasmids

Strains and plasmids are listed in Table S1. *S. aureus* strains were grown at 37°C in brain heart infusion broth. When necessary, chloramphenicol and erythromycin were added at 10 µg mL<sup>-1</sup>, and kanamycin was added at 200 µg mL<sup>-1</sup>.

### Genetic manipulations

Primers used for all the constructions are listed in Table S2. In pCN35Ω*sprA1*<sub>AS</sub>, SprA1<sub>AS</sub> sequence with 113 nts upstream and 26 nts downstream was amplified from Newman genomic DNA as a 215-bp fragment, with flanking PstI/EcoRI sites. The fragment is inserted in pCN35. In pCN35ΩST*sprA1/sprA1*<sub>AS</sub>, the *sprA1/sprA1*<sub>AS</sub> locus was amplified from Newman genomic DNA (with 48 upstream and 45 nt downstream) with streptotag<sup>16</sup> (46b aptamer with affinity to streptomycin) incorporated between *sprA1* and its promoter. For the truncated-flagged SprA1 construct, *sprA1* gene sequence, from positions -171 to +110, was amplified from Newman genomic as a 368-bp fragment flanked by PstI and EcoRI restriction sites in frame with the first 20 amino acids encoded within SprA1, the reverse primer contains 3XFlag (66-bp, 20 amino acids) followed by two UAG termination codons. The PCR fragment was inserted into pCN48<sup>29</sup> and then digested by PstI/NarI. The resulting 684-bp fragment (truncated *sprA1* ending by 3XFlag followed by the *blaZ* transcription

terminator) was inserted into pCN34<sup>29</sup>. The resulting amino acid sequence of the SprA1 fusion peptide is ‘MLIFVHIIAPVISGCAIAFDYKDHDGDYKDHDIDYKDDDDK’. The construction of the deletion mutant *S. aureus* strain Newman  $\Delta$ SprA1/SprA1<sub>AS</sub> was done as described<sup>30</sup>. Briefly, chromosomal gene disruption of *sprA1/sprA1<sub>AS</sub>* locus was constructed by deletion of targeted locus and insertion of erythromycin resistance gene by using the temperature-sensitive vector pBT2<sup>31</sup>.

### ***In vitro* transcription and RNA labeling**

All the RNAs used in this report were transcribed from PCR-amplified templates using Newman genomic DNA. Forward primers contain a T7 promoter sequence (Table S2). PCR generated DNA was used as template for transcription using the ‘Ambion T7Megascript’ kit. For synthesis of short RNAs (SprA1<sub>AS</sub>, 5’SprA1<sub>AS</sub>, 3’SprA1<sub>AS</sub>), template was produced by annealing the primers listed in Table S2. RNAs were gel purified, eluted passively and ethanol precipitated. 5' and 3' end labeling of the RNAs were performed as described<sup>13</sup>.

### **Primer extension, RACE mapping**

For SprA1<sub>AS</sub> 5' end mapping, RNA extracts from Newman pCN35 $\Omega$ *sprA1<sub>AS</sub>* were used. Primer extension carried out as described<sup>13</sup> using Superscript III reverse transcriptase. 5'-RACE of SprA1 were carried out as described<sup>13</sup>. Primers for end determination are listed in Table S2.

### **RNA Extraction and Northern Blots**

Isolated colonies were suspended in 5 ml of BHI and incubated at 37°C overnight. Culture was diluted 1:100 then incubated at 37°C with agitation and stopped at various phases of growth. RNA extraction was performed as described<sup>32</sup>. The DNA probes used to detect sRNA are listed in Table S2. Total RNA was separated on denaturing PAGE and transferred onto a Zeta probe GT membrane (Bio-Rad). Specific <sup>32</sup>P-labeled probes were hybridized with

ExpressHyb solution (Clontech) for 90 min, washed, exposed and scanned with a PhosphorImager (Molecular Dynamics).

### **Streptomycin-streptotag purification**

RNA extracts of Newman  $\Delta sprA1/sprA1_{AS}$  pCN35 $\Omega$ ST $sprA1/sprA1_{AS}$  are used for affinity purification. Streptomycin sepharose preparation and the affinity purification are performed as described<sup>16</sup>. Eluted RNAs are ethanol-precipitated.

### **Gel-mobility assays, structural probing and Toeprints**

Gel-mobility assays were performed as described<sup>13</sup>. RNAs mix were incubated in binding buffer (80 mM K-HEPES pH 7.5, 4 mM MgCl<sub>2</sub>, 330 mM KCl) before native gel separation. Structural assays were performed as described<sup>13</sup>. Structural analysis of duplexes between SprA1 and SprA1<sub>AS</sub> are prepared by incubating 0.5 pmol of labeled RNA with 1 pmol of unlabeled RNA in binding buffer 20 min at 30°C. Digestions with the various ribonucleases were performed for 15 min 30°C in the presence of 1 µg of total tRNA from yeast (V1 at 5.10<sup>-5</sup> units; S1 at 5 units, lead acetate at 0.75 mM). The toeprints were done as described<sup>30</sup> with modifications. *S. aureus* purified 70S were used and reverse transcription was performed using labeled primer 'sprA1Toep' (Table S2).

### **Protein extractions, western blots and *in vitro* translation assays.**

For proteins extractions during growth, the pellets were re-suspended in lysis buffer (50mM Tris-Cl pH7.5, 3mM MgCl<sub>2</sub>, 0.1 mg mL<sup>-1</sup> lysostaphin and 0.2U µL<sup>-1</sup> of Benzonase) incubated 15 minutes at 37°C then transferred into ice. Bradford assays were performed on the samples and equal amounts of total proteins were used for the Western Blots. The samples were separated on a 16% Tricine-SDS-PAGE<sup>33</sup>, transferred on Hybond™-P PVDF membrane (Amersham) and revealed using the Amersham™ ECL™ Plus detection Kit. *In vitro* translation using [<sup>35</sup>S]-methionine was performed using *E. coli* S30 extract system for linear templates (Promega) following the manufacturer's instruction. For the assays in the presence

of SprA1<sub>AS</sub> or other RNAs, the RNA mix was incubated in binding buffer 20min at 30°C. 30 pmol of purified WT SprA1 or SD-mutated SprA1 were used in the presence or absence of 60 pmol of SprA1<sub>AS</sub> or 300 pmol of either 5'SprA1<sub>AS</sub> or 3'SprA1<sub>AS</sub>. Samples were separated on a 16% Tricine-SDS-PAGE<sup>33</sup>. The gel was fixed, exposed and visualized with PhosphorImager.

### **Hemolytic assays**

For the titration of hemolytic activity of SprA1 peptide, 100µL of serial ½ dilutions of PBS containing peptides were pipetted in a V Bottom 96 Well Plate (Sigma). 100µL of PBS containing 3% (v/v) RBC are added to each well and incubated 1 hour at room temperature. For hemolysis comparison between human or sheep RBC, RBC were washed and diluted to 3% (v/v) in PBS. Human or sheep RBCs are incubated at 37°C with either 5µL of 50% (v/v) isopropanol (negative control) or with 5µL of 50% (v/v) isopropanol containing 3nmol of the chemically synthesized SprA1-encoded peptide.

### **Ribonucleotides, oligodesoxynucleotides and proteins**

SprA1 peptide was synthesized by PROTEOGENIX (Oberhausbergen, France). Superscript III reverse transcriptases, lysostaphin, Benzonase were purchased from Invitrogen. Restriction enzymes were from New England Biolabs (Beverly, MA). [ $\gamma$ <sup>32</sup>P]ATP, [ $\alpha$ <sup>32</sup>P]pCp (3000 mCi mmol<sup>-1</sup>) and [<sup>35</sup>S] methionine at (1150Ci mmol<sup>-1</sup> at 10mCi mL<sup>-1</sup>) were from Perkin-Elmer (Courtaboeuf, France).

### **ACKNOWLEDGMENTS**

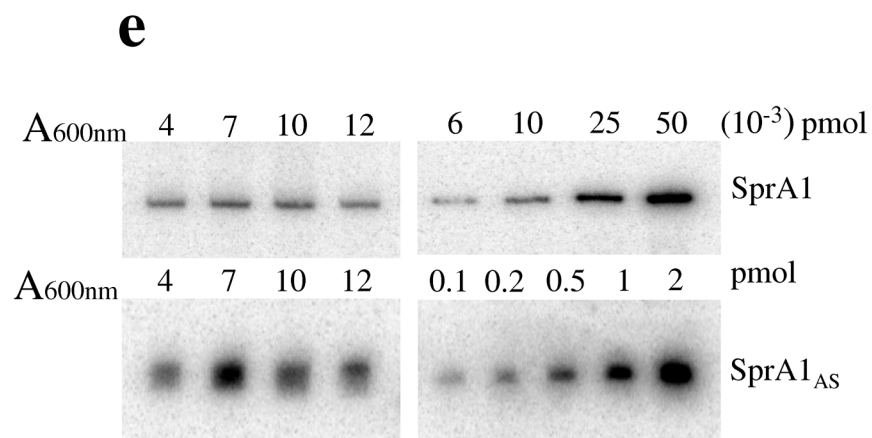
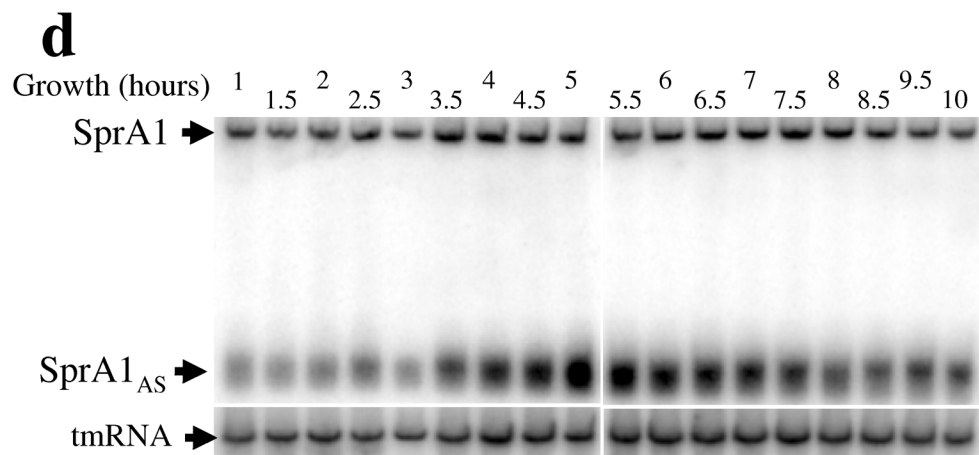
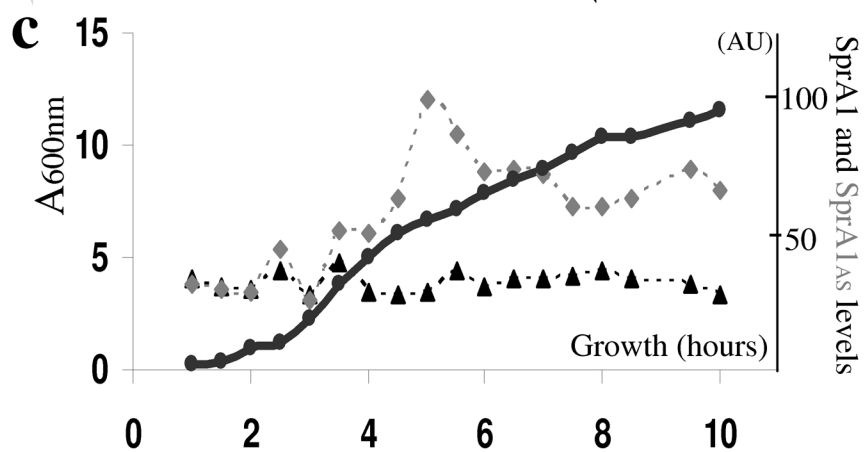
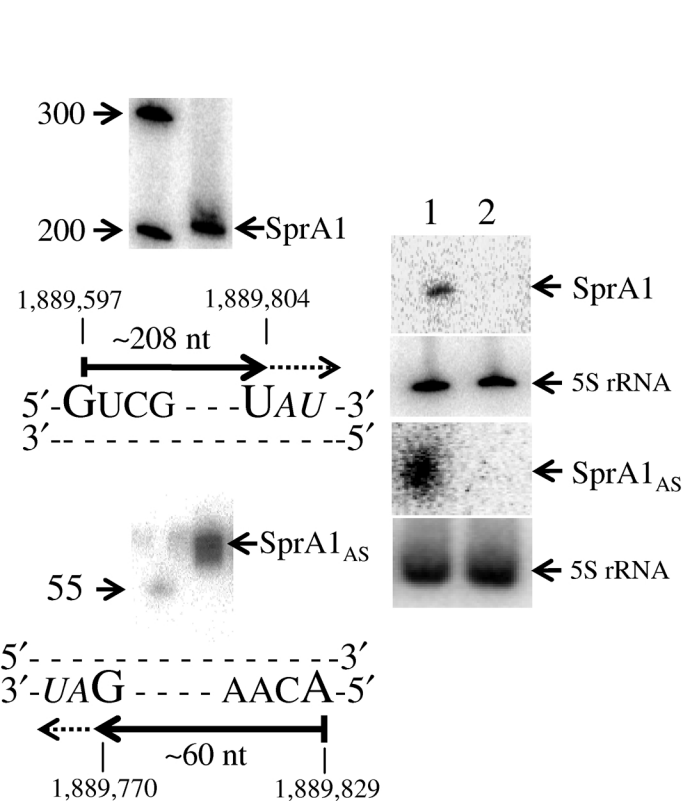
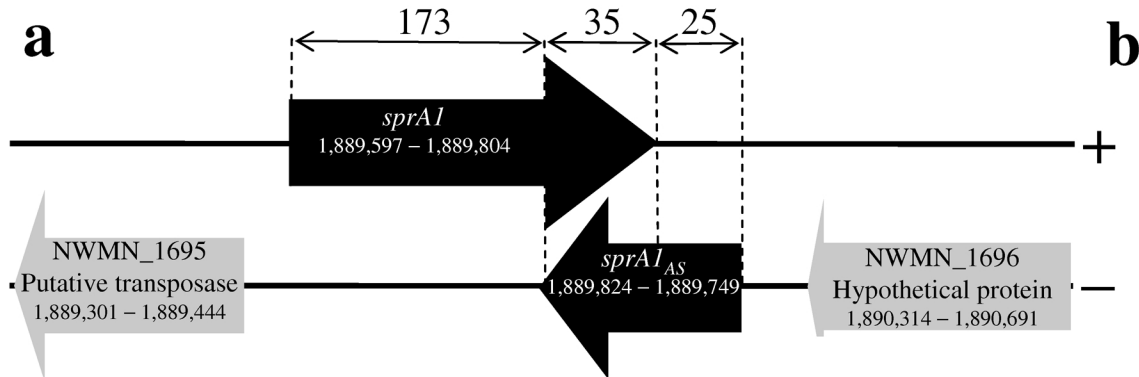
We are thankful to Drs S. Chabelskaya and M. Hallier for critical reading of the manuscript and comments. This study was supported by grant 'ANR-09-MIEN-030-01' from the 'Agence Nationale pour la Recherche' to B.F. and funds from the Inserm, Brittany region (Ph.D grant for N.S.) and from the French Department of Research and Education.

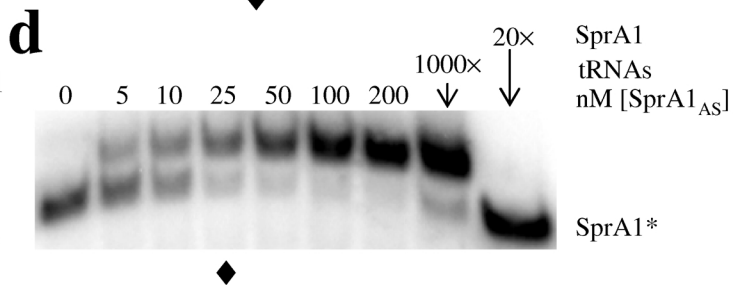
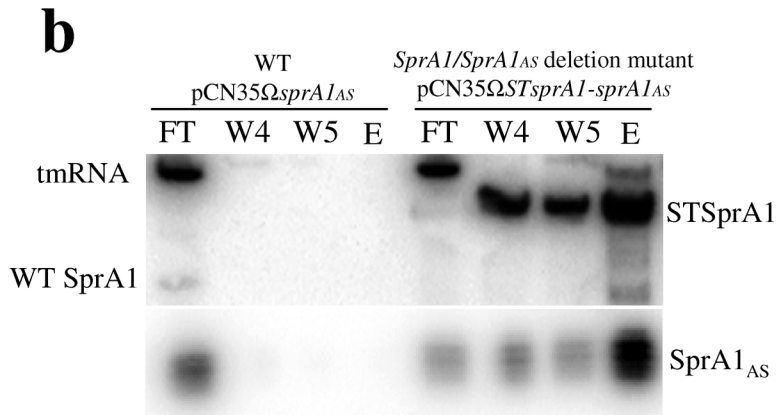
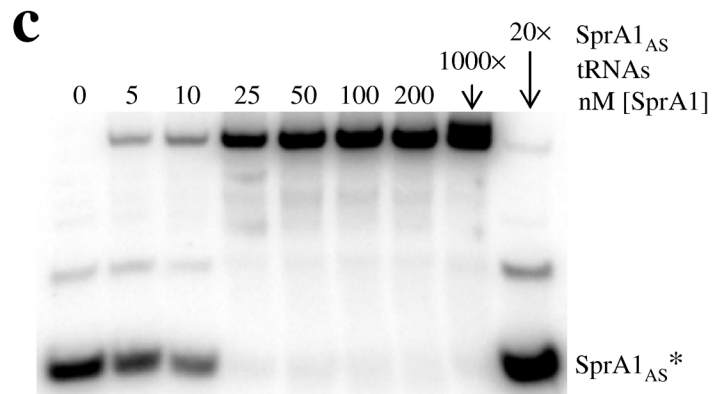
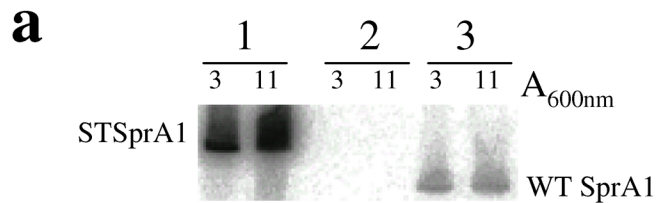
## **AUTHOR CONTRIBUTIONS**

N.S. and B.F. designed experiments, prepared samples, analyzed the data and wrote the manuscript. A.J. constructed the sRNA double mutant, the Hfq experiment and participated in discussions and manuscript writing.

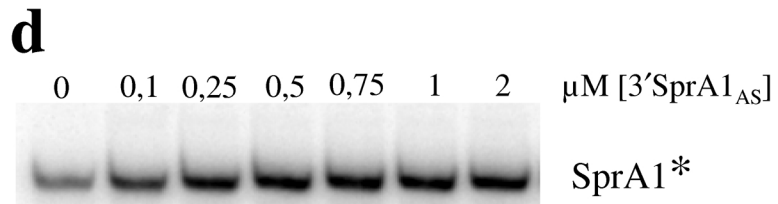
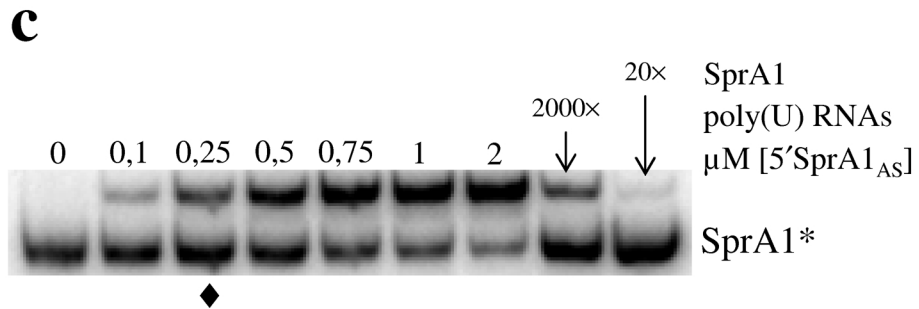
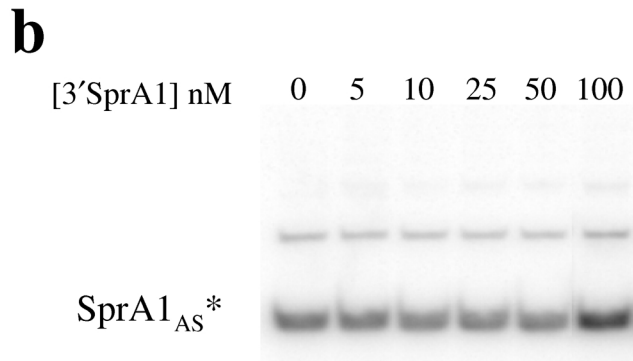
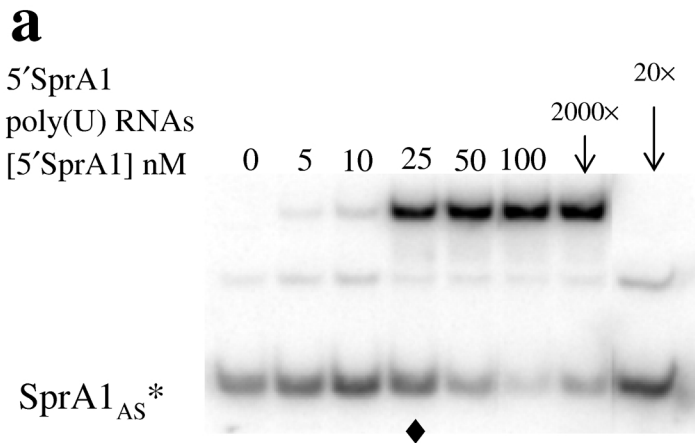
## **COMPETING FINANCIAL INTERESTS**

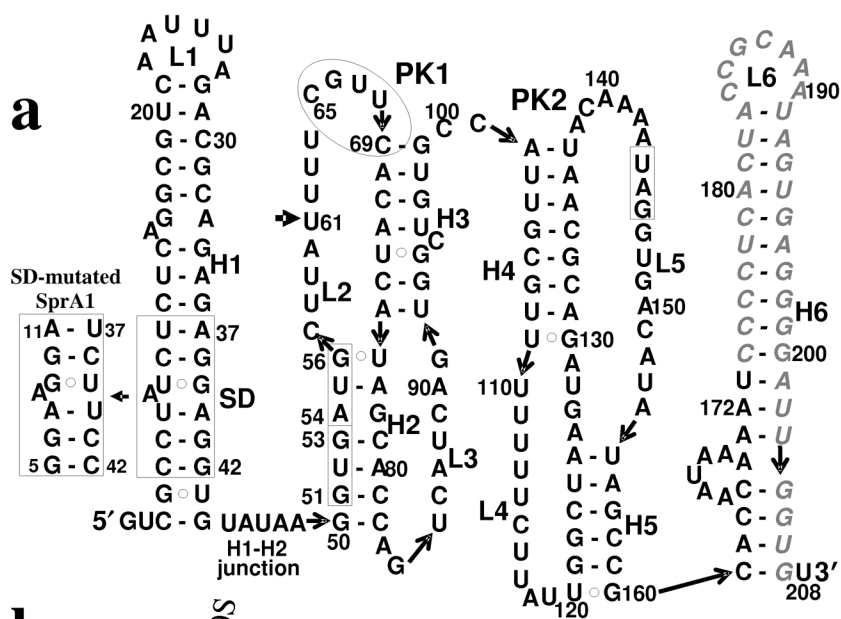
The authors declare no competing financial interests.



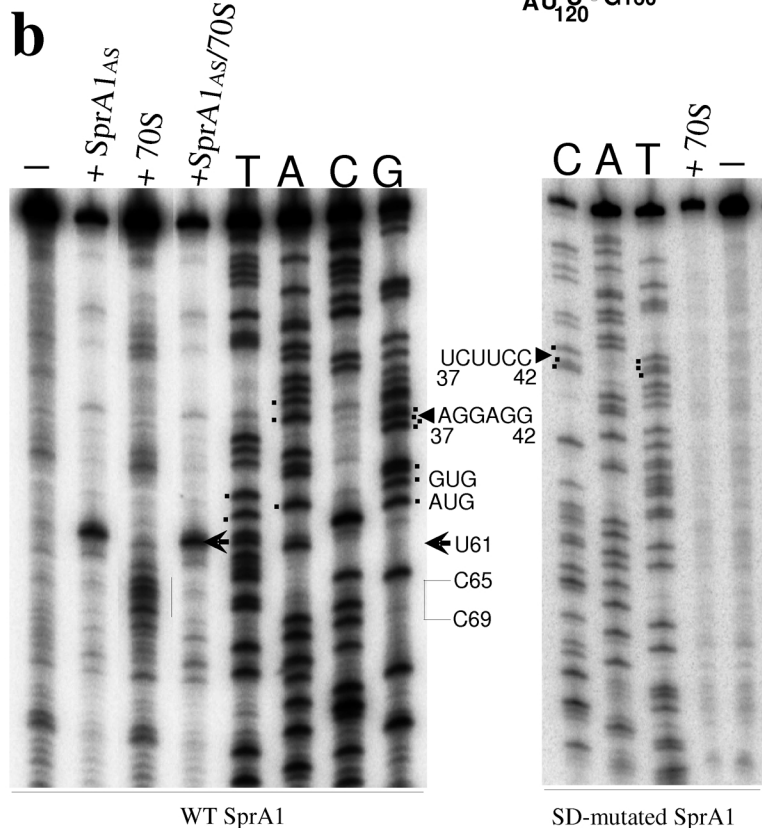
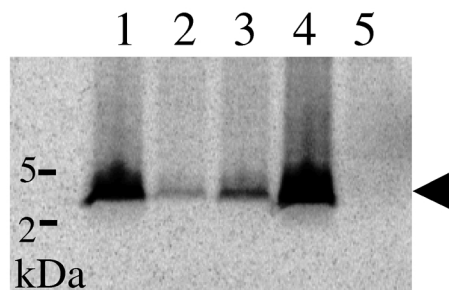








**c**



**d**

